# Synthesis, Crystal Structure, and Thermal Decomposition of Strontium Amidoborane

**ARTICLE** *in* THE JOURNAL OF PHYSICAL CHEMISTRY C · JANUARY 2010

Impact Factor: 4.77 · DOI: 10.1021/jp9097233



**7 AUTHORS**, INCLUDING:

Liuzhang Ouyang
South China University of Technology
**152** PUBLICATIONS **1,520** CITATIONS
SEE PROFILE

M. Zhu
South China University of Technology
**235** PUBLICATIONS **2,722** CITATIONS
SEE PROFILE

# Synthesis, Crystal Structure, and Thermal Decomposition of Strontium Amidoborane

**Qingan Zhang,*,† Chunxia Tang,† Chunheng Fang,† Fang Fang,‡ Dalin Sun,‡ Liuzhang Ouyang,§ and Min Zhu*,§**

*School of Materials Science and Engineering, Anhui University of Technology, Maanshan 243002, China, Department of Materials Science, Fudan University, Shanghai 200433, China, and School of Materials Science and Engineering, South China University of Technology, Guangzhou 510641, China*

*Received: October 10, 2009; Revised Manuscript Received: December 02, 2009*

Strontium amidoborane, $Sr(NH_2BH_3)_2$, is synthesized by gently milling the powder mixtures of $SrH_2$ and ammonia borane (in a 1:2 molar ratio), followed by isothermally processing the postmilled mixtures at 45 °C for 2 h. It is found that $Sr(NH_2BH_3)_2$ crystallizes with a monoclinic structure in space group $C2$, with lattice parameters $a = 8.1660(4)$ Å, $b = 5.0969(3)$ Å, $c = 6.7258(4)$ Å, and $\beta = 94.392(4)°$, and with $Z = 2$. In the structure, each $Sr^{2+}$ bonds with two $[NH_2BH_3]^{2-}$ ions with a Sr−N distance of 2.68 Å. Thermal analyses show that the decomposition of $Sr(NH_2BH_3)_2$ into $Sr(NBH)_2$ and $H_2$ initiates at about 60 °C and becomes violent as the temperature increases to 93 °C in the heating process at a rate of 2 °C $min^{-1}$. With the release of $H_2$, a considerable amount of $NH_3$ and small amounts of $B_2H_6$ are also emitted due to the decomposition of $Sr(NBH)_2$.

## Introduction

As a potential material for hydrogen storage, ammonia borane ($NH_3BH_3$) has attracted great attention over the past years because of its ideal combination of low molecular weight and high hydrogen content of 19.6 wt %. Upon heating to the temperature of 70−120 °C, $NH_3BH_3$ releases about 6.5 wt % of hydrogen gas with the formation of a complex polymeric aminoborane $(BH_2NH_2)_x$,[1−3] but this thermal decomposition is kinetically slow if $NH_3BH_3$ is not processed by ball-milling or doping with additives.[4−7] With an increase in temperature, the newly formed $(BH_2NH_2)_x$ releases more hydrogen gas, but concurrently gives rise to some other volatile species, such as diborane $B_2H_6$ and borazine $B_3N_3H_6$, that are detrimental and undesirable for fuel cell operation in automotive application.[2,3] Hence, recent studies have been focused on how to improve the dehydrogenation properties of $NH_3BH_3$ in terms of the reduced decomposition temperature, enhanced hydrogen release kinetics, and improved purity of hydrogen gas.[8−14]

As derivatives from $NH_3BH_3$, alkali metal amidoboranes, that is, $LiNH_2BH_3$ and $NaNH_2BH_3$, have been reported to vigorously release $H_2$ at about 90 °C free of borazine emission, in which the decomposition pathways for $LiNH_2BH_3$ and $NaNH_2BH_3$ are suggested to be $LiNBH+2H_2$ and $NaNBH+2H_2$, respectively.[15] However, these pathways have been argued by a subsequent reinvestigation work on $NaNH_2BH_3$,[16] which shows that a significant amount of ammonia ($NH_3$) is undesirably released accompanying hydrogen emission. Later on, an alkaline-earth metal amidoborane, $Ca(NH_2BH_3)_2$, has also been synthesized by the reaction of $NH_3BH_3$ with $CaH_2$ via a wet route using tetrahydrofuran (THF) as a solvent[17] or a ball-milling process.[18] $Ca(NH_2BH_3)_2$ has been reported to release $H_2$ at around 100 °C,[18] but the purity of the evolved hydrogen gas is unknown because the detailed analysis on the released gas from $Ca(NH_2BH_3)_2$ has not been given.[17,18] Hence, it remains unclear whether the $NH_3$ emission is generally present or not during the thermal decomposition of metal amidoboranes. The other question raised from the previous studies is that the measured hydrogen quantities released from these metal amidoboranes (especially in samples prepared by ball-milling) are much less than their theoretical values. For instance, $LiNH_2BH_3$ decomposes violently into LiNBH and $H_2$ at 90 °C,[15,18,19] but the measured amount of the hydrogen released rapidly from the ball-milled $LiNH_2BH_3$ sample is 70%,[19] and even only 50%,[18] of its theoretical value at 100 °C. Similarly, $Ca(NH_2BH_3)_2$ could theoretically give 4 equiv of $H_2$ after the decomposition into $Ca(NBH)_2$ and $H_2$ at 100 °C; however, only 2 equiv of $H_2$ are obtained from the ball-milled $Ca(NH_2BH_3)_2$ sample at 110 °C within 2 h.[18] Although the amounts of the gases released from the ball-milled samples increase and reach to their theoretical values with further raising the temperature from 110 to 200 °C,[18,19] this increment is assumed to be from the decomposition of LiNBH or $Ca(NBH)_2$,[17,20] rather than $LiNH_2BH_3$ or $Ca(NH_2BH_3)_2$. Therefore, it is necessary to clarify why the amounts of the hydrogen released from the ball-milled metal amidoboranes are lower than their theoretical values. Keeping these two questions in mind, we present herein the thermal decomposition features of a new alkaline-earth metal amidoborane, $Sr(NH_2BH_3)_2$.

In the present work, $Sr(NH_2BH_3)_2$ was carefully synthesized by two steps: First, the powder mixtures of $SrH_2$ and $NH_3BH_3$ were gently ball-milled to ensure good homogeneity. Unlike those previous investigations, the ball-milling process was carried out at a low temperature (about 0 °C), with the hope of avoiding or minimizing any thermally activated decomposition. After milling, the postmilled mixture was heated to 45 °C to enhance the solid−solid reaction between $SrH_2$ and $NH_3BH_3$ in order to maximize the yield of $Sr(NH_2BH_3)_2$. The crystal structure and thermal decomposition features of $Sr(NH_2BH_3)_2$ were subsequently examined by X-ray diffraction and thermal analyses. In addition to $H_2$, the emission of $NH_3$ was observed

* To whom correspondence should be addressed. E-mail: zhang03jp@yahoo.com.cn (Q.Z), memzhu@scut.edu.cn (M.Z.).
† Anhui University of Technology.
‡ Fudan University.
§ South China University of Technology.

10.1021/jp9097233 
Published on Web 01/05/2010

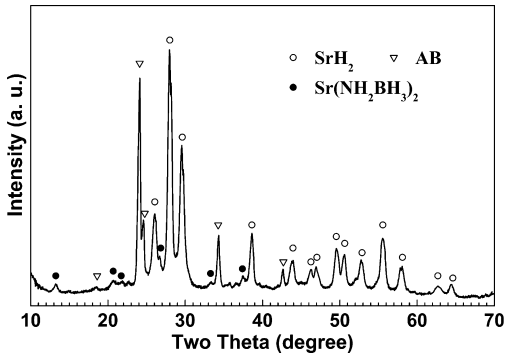


**Figure 1.** XRD pattern for the postmilled $SrH_2+2NH_3BH_3$ mixture.

during the $Sr(NH_2BH_3)_2$ decomposition, and the possible reason for the formation of $NH_3$ was discussed.

## Experimental Section

**Sample Preparation.** The starting powder materials, $SrH_2$ (99.5%, Soekawa Chemicals) and $NH_3BH_3$ (90%, Alfa Aesar), were purchased and used as received. The powders of $SrH_2$ and $NH_3BH_3$ in a molar ratio of 1:2 were mixed manually in a glovebox and then gently ball-milled under argon atmosphere (about 0.1 MPa). The ball-milling was performed using a QM-1SP2 planetary mill at a rotation speed of 150 rpm, with a stainless steel vial (80 $cm^3$) and balls (6 mm in diameter). The ball-to-powder weight ratio was 20:1. Prior to milling, the vial was first dipped into ice water for 2 h. The 5 min milling was then performed and repeated at 20 min intervals. During each interval, the vial was dipped into ice water to cool down. After the milling time was up to 1 h in total, the vial was again dipped into ice water for 1 h and then brought back to the glovebox. The milled samples were used for subsequent experiments immediately.

**Sample Characterization.** The reactions of $NH_3BH_3$ with $SrH_2$ were monitored using a simultaneous thermal analyzer (NETZSCH STA 409) equipped with a quadrupole mass spectrometer (QMS 403C). The differential thermal analysis (DTA), thermogravimetry (TG), and mass spectrometry (MS) measurements were performed under argon flow (30 mL $min^{-1}$) at a heating rate of 2 °C $min^{-1}$. The amounts of the released gases from the milled $SrH_2+2NH_3BH_3$ mixture were also measured using a calibrated Sieverts-type apparatus at 45 and 80 °C.

X-ray diffraction (XRD) measurements were carried out on a Rigaku D/Max 2500 VL/PC diffractometer with Cu Kα radiation at 50 kV and 150 mA. The XRD sample was loaded and sealed in a special homemade holder that can keep the sample under argon atmosphere in the course of the measurement. The software programs, TREOR90[21] and EXPO,[22,23] were first used to index the XRD pattern for $Sr(NH_2BH_3)_2$ and get the brief data about its crystallographic structure. Using these structural data as the starting model, the XRD pattern was further refined by the Rietveld program RIETAN-2000.[24]

## Results and Discussion

**Synthesis of $Sr(NH_2BH_3)_2$.** The XRD pattern for the postmilled $SrH_2+2NH_3BH_3$ mixture is shown in Figure 1 from which the following two features can be seen: (i) Most of the peaks are assigned to the starting materials, $SrH_2$ and $NH_3BH_3$, but some additional peaks appear. These additional peaks come from $Sr(NH_2BH_3)_2$ that was formed by the reaction between $SrH_2$ and $NH_3BH_3$, namely

$$SrH_2 + 2NH_3BH_3 \rightarrow Sr(NH_2BH_3)_2 + 2H_2 \quad (1)$$

which will be further discussed below. (ii) Though the ball-milling process in the present study was carefully carried out at rather low temperature and low speed, a hump appears in the background, identical to the scenarios as previously reported in the syntheses of $LiNH_2BH_3$, $NaNH_2BH_3$, and $Ca(NH_2BH_3)_2$.[15,16,18] The appearance of the hump suggests that the newly formed $Sr(NH_2BH_3)_2$ starts to decompose and its decomposition products are in an amorphous state. Additional experiments show that further increases in milling time, milling speed, and temperature enhance not only the formation of $Sr(NH_2BH_3)_2$ but also its decomposition (Figures SI-2 and SI-3, Supporting Information). Therefore, it seems that the decomposition of alkaline-earth metal amidoborane is difficult to be avoided if it is synthesized by the method of ball-milling. This explains why the measured amount of the hydrogen released from the $Ca(NH_2BH_3)_2$ sample prepared by ball-milling is much less than its theoretical value at the decomposition temperature.[18]

The DTA/TG profiles for the postmilled $SrH_2+2NH_3BH_3$ mixture in the heating process at a rate of 2 °C $min^{-1}$ is shown in Figure 2a. It can be seen from the DTA curve that there are two prominent exothermic peaks centered at about 58 and 93 °C and the first peak starting at 40 °C overlaps, in part, with the second one. This means that at least two exothermic reactions occur in this temperature range. The simultaneous MS analysis of the gases released in the heating process is displayed in Figure 2b that confirms the two-step reactions observed in Figure 2a. Similar to the $CaH_2-NH_3BH_3$ system,[18] the two-step reactions correspond to the formation and decomposition of $Sr(NH_2BH_3)_2$, respectively. Note that $NH_3$ and $B_2H_6$ are clearly present, accompanied with $H_2$ as the temperature is over

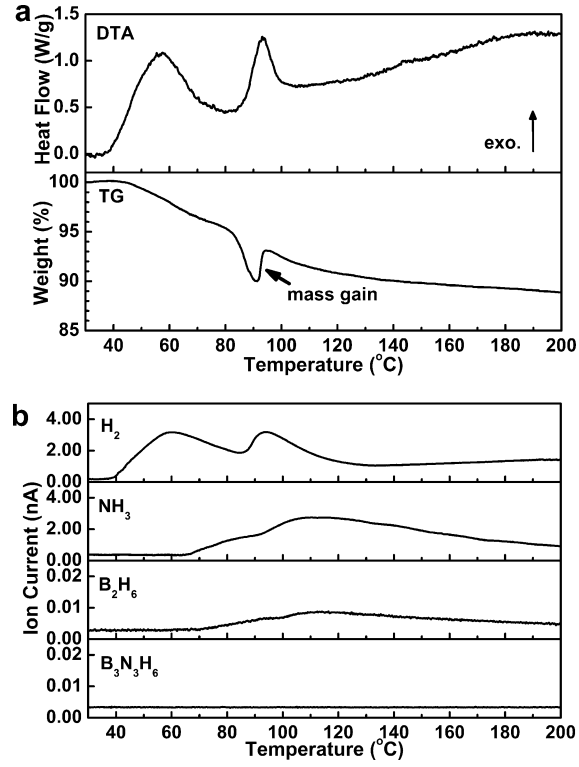


**Figure 2.** Simultaneous DTA/TG (a) and MS (b) analysis of the released gas during the reactions of the postmilled $SrH_2+2NH_3BH_3$ mixture at a heating rate of 2 °C $min^{-1}$. The mass gain in the TG curve is possibly attributed to some products or intermediates that are formed by the side reaction involving the released $H_2$ and $NH_3$ present in the sample environment.

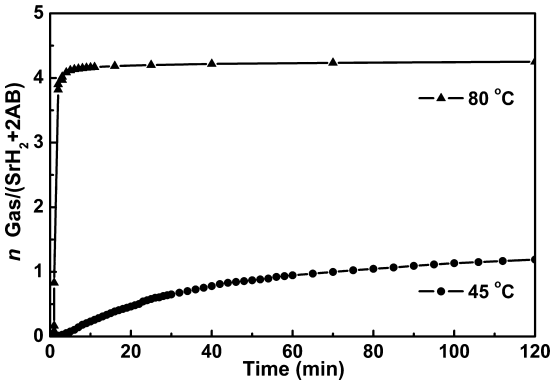


**Figure 3.** Time dependence of the released gas from the postmilled $SrH_2+2NH_3BH_3$ mixture at 45 and 80 °C.

65 °C. This is consistent with the results observed in the heating process of $NaNH_2BH_3$.[16] Moreover, it should be mentioned that the $NH_3$ release is not synchronous with the hydrogen release, indicating that the $NH_3$ is not generated by the two-step reactions. The reason for the $NH_3$ emission will be discussed below. The TG curve shows that the total mass loss is about 11.2% up to 200 °C. However, a mass gain appears noticeably at around 90 °C and lasts for about 5 min, as arrowed in the TG curve. The exact reason for this mass gain is presently unclear, but possibly attributes to some products or intermediates that are formed by the side reaction involving the released $H_2$ and $NH_3$ present in the sample environment.

To increase the yield of $Sr(NH_2BH_3)_2$, the postmilled $SrH_2+2NH_3BH_3$ mixture was first vacuumed at room temperature and then isothermally processed at 45 °C for 2 h. Though the synthesis reaction at 45 °C is kinetically slow, the decomposition of freshly formed $Sr(NH_2BH_3)_2$ can be avoided in terms of Figure 2a. This is further confirmed by conducting the emitted gas into a Nessler's reagent where $NH_3$ is not detected. Moreover, the sublimation of ammonia borane at 45 °C is negligible in terms of the results reported recently by Palumbo et al.[25] Therefore, it is safe to consider that only hydrogen is released in the isothermal process. The time dependence of the released $H_2$ during the isothermal treatment is present in Figure 3, showing that about 1.2 equiv of $H_2$ per ($SrH_2+2NH_3BH_3$) is obtained in 2 h; that means about 0.6 equiv of $Sr(NH_2BH_3)_2$ per ($SrH_2+2NH_3BH_3$) is simultaneously formed, according to reaction 1. The yield of $Sr(NH_2BH_3)_2$ is lower than the theoretical value by 0.4 equiv. This is reasonable, given that, (i) prior to the isothermal treatment, the formation and decomposition of $Sr(NH_2BH_3)_2$ partially occurred in the previous ball-milling process and (ii) some of the $SrH_2$ and $NH_3BH_3$ were unreacted during the isothermal treatment.

**Crystal Structure of $Sr(NH_2BH_3)_2$.** The XRD pattern for $Sr(NH_2BH_3)_2$ is indexed to be a monoclinic unit cell in space group $C2$ (No. 5). The cell parameters are determined to be $a$ = 8.1660(4) Å, $b$ = 5.0969(3) Å, $c$ = 6.7258(4) Å, and $\beta$ = 94.392(4)°. During the Rietveld refinement, the Sr coordinate (0 $y$ 0) was fixed as the origin (0 0 0) for avoiding the origin floating along the $y$ axis. The refined coordinates of non-hydrogen atoms are listed in Table 1. Although $Sr(NH_2BH_3)_2$ crystallizes in the same space group $C2$ as $Ca(NH_2BH_3)_2$,[18] their atomic coordinates are quite different from each other. As X-ray is not sensitive to hydrogen, the atomic coordinates for H atoms are not determined in the present work. Thus, the characteristics of B−H and N−H bonds in $Sr(NH_2BH_3)_2$ are unknown yet. Further studies on the structure of the deuteried $Sr(NH_2BH_3)_2$ by means of neutron diffraction are in progress.

**TABLE 1: Atomic Sites, Occupancy, Coordinates, and Isotropic Thermal Parameters for $Sr(NH_2BH_3)_2$ Refined from X-ray Powder Diffraction Data[a]**

| atom | site | $g$ | $x$ | $y$ | $z$ | $U_{iso}$ (Å$^2$) |
|---|---|---|---|---|---|---|
| Sr | 2$a$ | 1 | 0 | 0 | 0 | 0.013(2) |
| N | 4$c$ | 1 | 0.382(1) | 0.263(2) | 0.315(2) | 0.019(5) |
| B | 4$c$ | 1 | 0.353(1) | 0 | 0.209(2) | 0.008(5) |

[a] Space group, $C2$ (No. 5); cell parameters, $a$ = 8.1660(4) Å, $b$ = 5.0969(3) Å, $c$ = 6.7258(4) Å, and $\beta$ = 94.392(4)°; $Z$ = 2; $R_{wp}$ = 7.21%; $R_p$ = 5.70%; and $S$ = 2.61. The Sr coordinate (0 $y$ 0) was fixed as the origin (0 0 0). In this case, the $y$ value of the B coordinate ($x$ $y$ $z$) is very close to zero, and thus, the $y$ value was also fixed to be $y$ = 0. The positions of the H atoms were not determined.

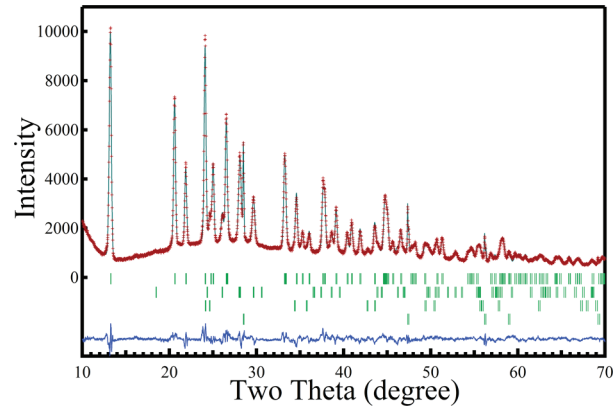


**Figure 4.** Rietveld refinement of the XRD pattern for $Sr(NH_2BH_3)_2$ obtained after gas release of the postmilled $SrH_2+2NH_3BH_3$ mixture at 45 °C for 2 h. The vertical bars (from above) indicate the positions of the Bragg diffraction for $Sr(NH_2BH_3)_2$, $SrH_2$, $NH_3BH_3$, and the internal reference Si, respectively.

Figure 4 shows the observed and calculated XRD patterns of the synthesized $Sr(NH_2BH_3)_2$ sample with the addition of 5 wt % standard Si as internal reference. It can be seen that the refined pattern fits the observed one very well. The Rietveld analysis gives that, among the crystalline phases, the relative amounts of $Sr(NH_2BH_3)_2$, $SrH_2$, $NH_3BH_3$, and Si are 77, 10, 6, and 7 wt %, respectively. When these values are normalized to the actual mass of standard Si, the phase abundance of the $Sr(NH_2BH_3)_2$, $SrH_2$, and $NH_3BH_3$ can be determined, respectively, to be 55, 7, and 4 wt %; thus, that of the amorphous phase is 34 wt % in the synthesized sample. Note that the amount of $Sr(NH_2BH_3)_2$ obtained here complies with the quantity of released $H_2$ measured by the volumetric method in Figure 3.

The crystal structure of $Sr(NH_2BH_3)_2$ is illustrated in Figure 5. In the structure, each $Sr^{2+}$ ion bonds with two $[NH_2BH_3]^{2-}$ ions, with a Sr−N distance of 2.68 Å. This value is close to those in $SrN_2$ (2.531−2.765 Å)[26] and SrNH (2.590−3.131 Å).[27] The B−N bond length in $Sr(NH_2BH_3)_2$ is 1.53 Å, slightly shorter than 1.58 Å in $NH_3BH_3$,[28,29] but agrees with 1.547 Å in $LiNH_2BH_3$ and 1.546 Å in $Ca(NH_2BH_3)_2$.[18] This suggests that the B−N bonding is stronger in the alkali and alkaline-earth metal amidoboranes than in $NH_3BH_3$.[18,30]

**Decomposition of $Sr(NH_2BH_3)_2$.** As shown in Figure 2a, the second exothermic peak partially overlaps with the first one, indicating that the onset decomposition temperature of $Sr(NH_2BH_3)_2$ is only slightly higher than its formation temperature. This is the reason why the decomposition occurs readily accompanying the formation of $Sr(NH_2BH_3)_2$ during ball-

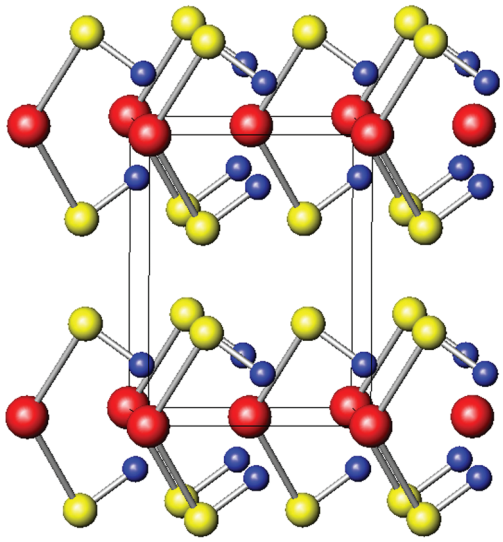

**Figure 5.** Crystal structure of $Sr(NH_2BH_3)_2$ viewed approximately along the *x* axis (*z* is vertical). The Sr, N, and B atoms are, respectively, represented as red, yellow, and blue spheres. The positions of H atoms are not determined.

milling. To determine the decomposition temperature for $Sr(NH_2BH_3)_2$, the simultaneous DTA/TG/MS analysis on the $Sr(NH_2BH_3)_2$ sample prepared by isothermally processing the postmilled $SrH_2+2NH_3BH_3$ mixture at 45 °C for 2 h was carried out and shown in Figure 6. On comparison with Figure 2a, it can be seen that the peak corresponding to the formation of $Sr(NH_2BH_3)_2$ disappears, but the one corresponding to the decomposition of $Sr(NH_2BH_3)_2$ exists and starts at 60 °C. However, the DTA and TG curves in Figure 6a show that the decomposition rate of $Sr(NH_2BH_3)_2$ is slow at 60 °C. This result is also proven by the XRD pattern given in Figure 7 that shows some of the $Sr(NH_2BH_3)_2$ remains in the sample obtained after gas release at 60 °C. To enhance the reaction, the postmilled $SrH_2+2NH_3BH_3$ mixture was processed isothermally at 80 °C, and the time dependence of the released gas was measured and is shown Figure 3. It can be seen that the reaction of $NH_3BH_3$ with $SrH_2$ is rapid at 80 °C under isothermal conditions.

Analogous to the cases of $LiNH_2BH_3$, $NaNH_2BH_3$, and $Ca(NH_2BH_3)_2$,[15,18] the thermal decomposition of $Sr(NH_2BH_3)_2$ may be written as

$$Sr(NH_2BH_3)_2 \rightarrow Sr(NBH)_2 + 4H_2 \qquad (2)$$

Hence, the overall reaction of $NH_3BH_3$ with $SrH_2$ at 80 °C under isothermal conditions should be the combination of reactions 1 and 2, namely

$$SrH_2 + 2NH_3BH_3 \rightarrow Sr(NBH)_2 + 6H_2 \qquad (3)$$

Reaction 3 is supported by the XRD pattern (see Figure 7) of the sample prepared at 80 °C in which the $Sr(NH_2BH_3)_2$ is not detected, except for the strong scattering in the background (because $Sr(NBH)_2$ is in an amorphous state) and some unreacted $SrH_2$. Note that only about 4.3 equiv of gas per $(SrH_2+2NH_3BH_3)$ is released from the milled mixture at 80 °C (see Figure 3), which is less than the value of 6 equiv given by reaction 3. This is due to the fact that $Sr(NH_2BH_3)_2$ and its decomposition product were partially formed during ball-milling prior to the isothermal treatment at 80 °C.

Importantly, as shown in Figure 6a, the amount of released gas increases with further raising the temperature up to 200 °C, but the mass loss reaches 9.9 wt %, which is higher than the

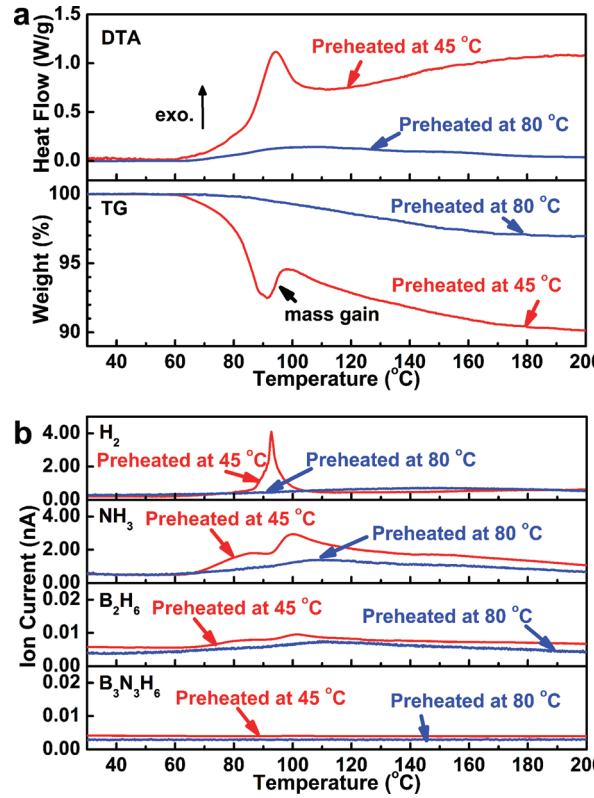


**Figure 6.** Simultaneous DTA/TG (a) and MS (b) analyses of the released gases from the samples obtained after gas release of the postmilled $SrH_2+2NH_3BH_3$ mixture at 45 °C (red) and 80 °C (blue) for 2 h, respectively. The mass gain in the TG curve is possibly attributed to some products or intermediates that are formed by the side reaction involving the released $H_2$ and $NH_3$ present in the sample environment.

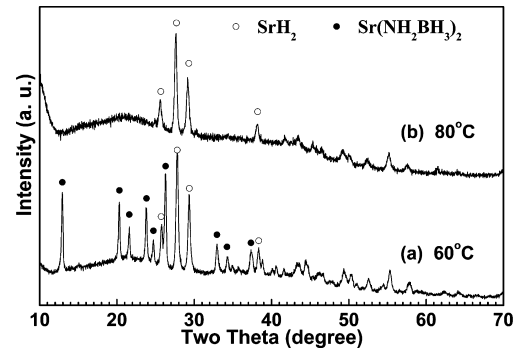


**Figure 7.** XRD patterns for the samples obtained after gas release at 60 and 80 °C for 2 h.

theoretical hydrogen content of 6.8 wt % for $Sr(NH_2BH_3)_2$. Thus, it is reasonable to deduce that, in addition to $H_2$, there are some other species existing in the released gas. In support of this deduction, the MS analysis shown in Figure 6b indicates clearly the release of $NH_3$ together with small amounts of $B_2H_6$ starting at 65 °C, occurring both prior and posterior to the vigorous hydrogen release at 93 °C. The $NH_3$ released in this temperature range is also identified by conducting the outlet gas into a Nessler's reagent.[31]

**Reason for $NH_3$ Emission.** Similar to the decomposition pathway of ammonia borane,[32] the decomposition of $Sr(NH_2BH_3)_2$ is actually not so simple, but more complicated, than that of reaction 2. For example, as a product, $NH_3$ is observed but not included in reaction 2. To explain the $NH_3$ emission in the case of $NaNH_2BH_3$, Fijalkowskia et al.

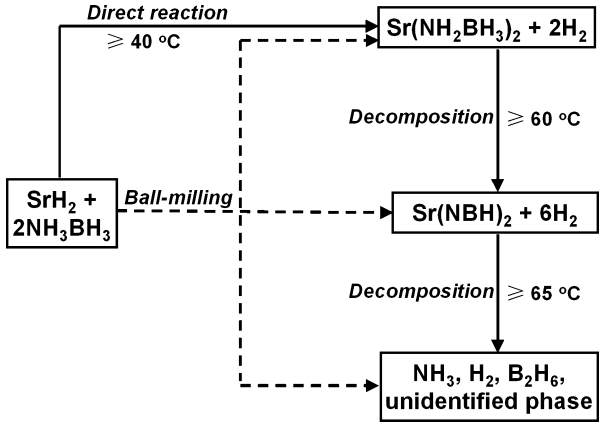


**Figure 8.** Schematic representation of the chemical reactions in the $SrH_2-NH_3BH_3$ system.

speculated that, prior to the decomposition, $NaNH_2BH_3$ may dimerize to an ionic form $[NH_3Na]^+[BH_3(NHNa)BH_3]^-$ and this ionic species is unstable and easily releases $NH_3$.[16] However, this speculation does not fully comply with the case of $Sr(NH_2BH_3)_2$ because the release of $NH_3$ is observed not only prior to but also posterior to the decomposition.

To understand the reason for the $NH_3$ emission, the simultaneous DTA/TG/MS data of the sample prepared by isothermally processing the postmilled $SrH_2+2NH_3BH_3$ mixture at 80 °C for 2 h were measured and compared in Figure 6. A broad exothermic peak is observed in the temperature range of 65−200 °C. This peak must exist previously, but due to its weak intensity, it is masked by the strong peak at 93 °C for the sample preheated at 45 °C for 2 h. This weak peak corresponds to the release of $NH_3$ accompanied with small amounts of $B_2H_6$ and $H_2$, showing a mass loss of 3% from 65 to 200 °C. This means that the $NH_3$ arises from the decomposition of the amorphous $Sr(NBH)_2$. The $NH_3$ gas released prior to the vigorous release of hydrogen at 93 °C from the sample preheated at 45 °C for 2 h is caused by the decomposition of the amorphous $Sr(NBH)_2$ formed in the ball-milling process and the heating process from 60 to 93 °C, whereas that released posterior to the vigorous release of hydrogen is mainly from the $Sr(NBH)_2$ formed at 93 °C. Although the decomposition mechanism of $Sr(NBH)_2$ is presently unclear, the gaseous $NH_3$, $B_2H_6$, and $H_2$ and some unidentified solid phases are detected to be its decomposition products (see Figure SI-4, Supporting Information).

The principal reactions occurring in the $SrH_2-NH_3BH_3$ system during ball-milling and thermal decomposition can be outlined in Figure 8, in terms of the results obtained in the present work. As indicated by the solid lines, $NH_3BH_3$ reacts directly with $SrH_2$ to form $Sr(NH_2BH_3)_2$ and $H_2$ starting at 40 °C, and $Sr(NH_2BH_3)_2$ begins to decompose into $Sr(NBH)_2$ and $H_2$ as the temperature reaches 60 °C. Further increasing the temperature to 65 °C, $Sr(NBH)_2$ decomposes to generate $NH_3$, $B_2H_6$, and $H_2$ as well as some unidentified solid-state phases. During the ball-milling of the $SrH_2+2NH_3BH_3$ mixture, as illustrated by the dashed lines in Figure 8, the decomposition reactions may take place along with the formation of $Sr(NH_2BH_3)_2$, identical to the results reported in the synthesis of $NaNH_2BH_3$ via ball-milling of the $NaH+NH_3BH_3$ mixture.[16] It is worthy noting that the decomposition of $Sr(NBH)_2$ readily occurs with the vigorous decomposition of $Sr(NH_2BH_3)_2$ in the heating process, thus exploring an efficient way to inhibit the $NH_3$ emission during the dehydrogenation of $Sr(NH_2BH_3)_2$ is a key issue in the following effort.

## Conclusions

The present work shows that $Sr(NH_2BH_3)_2$ can be synthesized by isothermally processing the gently ball-milled $SrH_2+2NH_3BH_3$ mixture at 45 °C. However, both $Sr(NH_2BH_3)_2$ and its decomposition product partially form during the ball-milling process, leading to the decrease in the yield of $Sr(NH_2BH_3)_2$. This suggests that alternative methods, instead of ball-milling, for the syntheses of metal amidoboranes should be developed in order to achieve a higher yield. $Sr(NH_2BH_3)_2$ crystallizes with a monoclinic structure in space group $C2$, with cell parameters $a = 8.1660(4)$ Å, $b = 5.0969(3)$ Å, $c = 6.7258(4)$ Å, and $\beta = 94.392(4)°$, and with $Z = 2$. In the structure, each $Sr^{2+}$ bonds with two $[NH_2BH_3]^{2-}$ ions with a Sr−N distance of 2.68 Å. $Sr(NH_2BH_3)_2$ decomposes into $Sr(NBH)_2$ and $H_2$, starting at about 60 °C, but the decomposition reaction is kinetically slow at the onset temperature. The thermal decomposition becomes violent when the temperature increases to about 80 °C under isothermal conditions or 93 °C in the heating process at a rate of 2 °C $min^{-1}$. However, a considerable amount of $NH_3$ and small amounts of $B_2H_6$ are also released during the thermal decomposition. The release of $NH_3$ and $B_2H_6$ is caused by the decomposition of the amorphous $Sr(NBH)_2$. These results provide us new information on the understanding of the decomposition mechanism of metal amidoboranes.

**Acknowledgment.** This work was financially supported by the Ministry of Science and Technology of China (Nos. 2007AA05Z113 and 2010CB631302) and the National Natural Science Foundation of China (Nos. 20833009 and 50925102).

**Supporting Information Available:** XRD patterns for the $SrH_2+2NH_3BH_3$ mixtures before ball-milling (Figure SI-1) and after the ball-milling at 300 rpm (Figures SI-2 and SI-3) and for the sample obtained after heating the postmilled $SrH_2+2NH_3BH_3$ mixture from 30 to 200 °C at a rate of 2 °C $min^{-1}$ (Figure SI-4). This material is available free of charge via the Internet at http://pubs.acs.org.

## References and Notes

(1) Wolf, G.; Baumann, J.; Baitalow, F.; Hoffmann, F. P. *Thermochim. Acta* **2000**, *343*, 19–25.
(2) Baitalowa, F.; Baumann, J.; Wolf, G.; Jaenicke-Robler, K.; Leitner, G. *Thermochim. Acta* **2002**, *391*, 159–168.
(3) Baumann, J.; Baitalow, F.; Wolf, G. *Thermochim. Acta* **2005**, *430*, 9–14.
(4) Paul, A.; Musgrave, C. B. *Angew. Chem., Int. Ed.* **2007**, *46*, 8153–8156.
(5) Shaw, W. J.; Linehan, J. C.; Szymczak, N. K.; Heldebrant, D. J.; Yonker, C.; Camaioni, D. M.; Baker, R. T.; Autrey, T. *Angew. Chem., Int. Ed.* **2008**, *47*, 1–5.
(6) Keaton, R. J.; Blacquiere, J. M.; Baker, R. T. *J. Am. Chem. Soc.* **2007**, *129*, 1844–1845.
(7) He, T.; Xiong, Z.; Wu, G.; Chu, H.; Wu, C.; Zhang, T.; Chen, P. *Chem. Mater.* **2009**, *21*, 2315–2318.
(8) Li, L.; Yao, X.; Sun, C.; Du, A.; Cheng, L.; Zhu, Z.; Yu, C.; Zou, J.; Smith, S. C.; Wang, P.; Cheng, H. M.; Frost, R. L.; Lu, G. Q. *Adv. Funct. Mater.* **2009**, *19*, 265–271.
(9) Peng, B.; Chen, J. *Energy Environ. Sci.* **2008**, *1*, 479–483.
(10) Heldebrant, D. J.; Karkamkar, A.; Hess, N. J.; Bowden, M.; Rassat, S.; Zheng, F.; Rappe, K.; Autrey, T. *Chem. Mater.* **2008**, *20*, 5332–5336.
(11) Blaquiere, N.; Diallo-Garcia, S.; Gorelsky, S. I.; Black, D. A.; Fagnou, K. *J. Am. Chem. Soc.* **2008**, *130*, 14034–14035.
(12) Dietrich, B. L.; Goldberg, K. I.; Heinekey, D. M.; Autrey, T.; Linehan, J. C. *Inorg. Chem.* **2008**, *47*, 8583–8585.
(13) Paolone, A.; Palumbo, O.; Rispoli, P.; Cantelli, R.; Autrey, T. *J. Phys. Chem. C* **2009**, *113*, 5872–5878.
(14) Paolone, A.; Palumbo, O.; Rispoli, P.; Cantelli, R.; Autrey, T.; Karkamker, A. *J. Phys. Chem. C* **2009**, *113*, 10319–10321.
(15) Xiong, Z.; Yong, C. K.; Wu, G.; Chen, P.; Shaw, W.; Karkamkar, A.; Autrey, T.; Jones, M. O.; Johnson, S. R.; Edwards, P. P.; David, W. I. F. *Nat. Mater.* **2008**, *7*, 138–141.

(16) Fijalkowskia, K. J.; Grochala, W. *J. Mater. Chem.* **2009**, *19*, 2043–2050.
(17) Diyabalanage, H. V. K.; Shrestha, R. P.; Semelsberger, T. A.; Scoot, B. L.; Bowden, M. E.; Davis, B. L.; Burrell, A. K. *Angew. Chem., Int. Ed.* **2007**, *46*, 8995–8997.
(18) Wu, H.; Zhou, W.; Yildirim, T. *J. Am. Chem. Soc.* **2008**, *130*, 14834–14839.
(19) Kang, X.; Fang, Z.; Kong, L.; Cheng, H.; Yao, X.; Lu, G.; Wang, P. *Adv. Mater.* **2008**, *20*, 2756–2759.
(20) Xiong, Z.; Wu, G.; Chua, Y. S.; Hu, J.; He, T.; Xu, W.; Chen, P. *Energy Environ. Sci.* **2008**, *1*, 360–363.
(21) Werner, P. E.; Eriksson, L.; Westdahl, M. *J. Appl. Crystallogr.* **1985**, *18*, 367–370.
(22) Altomare, A.; Burla, M. C.; Cascarano, G.; Giacovazzo, C.; Guagliardi, A.; Moliterni, A. G. G.; Polidori, G. *J. Appl. Crystallogr.* **1995**, *28*, 842–846.
(23) Altomare, A.; Cascarano, G.; Giacovazzo, C.; Guagliardi, A.; Burla, M. C.; Polidori, G.; Camalli, M. *J. Appl. Crystallogr.* **1994**, *27*, 435–436.
(24) Izumi, F.; Ikeda, T. *Mater. Sci. Forum* **2000**, *321/323*, 198–203.
(25) Palumbo, O.; Paolone, A.; Rispoli, P.; Cantelli, R.; Autrey, T. *J. Power Sources* **2010**, *195*, 1615–1618.
(26) Auffermann, G.; Prots, Y.; Kniep, R. *Angew. Chem., Int. Ed.* **2001**, *40*, 547–549.
(27) Schultz-Coulon, V.; Irran, E.; Putz, B.; Schnick, W. *Z. Anorg. Allg. Chem.* **1999**, *625*, 1086–1092.
(28) Miranda, C. R.; Ceder, G. *J. Chem. Phys.* **2007**, *126*, 184703.
(29) Hess, N. J.; Schenter, G. K.; Hartman, M. R.; Daemen, L. L.; Proffen, T.; Kathmann, S. M.; Mundy, C. J.; Hartl, M.; Heldebrant, D. J.; Stowe, A. C.; Autrey, T. *J. Phys. Chem. A* **2009**, *113*, 5723–5735.
(30) Lee, T. B.; McKee, M. L. *Inorg. Chem.* **2009**, *48*, 7564–7575.
(31) Chen, P.; Xiong, Z.; Luo, J.; Lin, J.; Tan, K. L. *Nature* **2002**, *420*, 302–304.
(32) Stowe, A. C.; Shaw, W. J.; Linehan, J. C.; Schmid, B.; Autrey, T. *Phys. Chem. Chem. Phys.* **2007**, *9*, 1831–1836.

JP9097233